Prepared for submission to JINST

PET Electronics & Technologies 2023 - PETtech23
12-13 September, 2023
Duisburg, Germany

On estimating the effective sensitivity of a TOF-PET system for a particular imaging task

J. Nuyts,[a,1] **S. A. Zaman Pour**[a] **S. Noë**[a] **G. Schramm**[a] **A. Rezaei**[a]

[a] *KU Leuven, University of Leuven, Department of Imaging and Pathology, Nuclear Medicine & Molecular imaging; Medical Imaging Research Center (MIRC), B-3000, Leuven, Belgium*

E-mail: johan.nuyts@uzleuven.be

Abstract: Comparing positron emission tomography (PET) systems which have different features is not straightforward. To address this, we propose to image the same object with all considered PET systems using a fixed scan time, and reconstruct from each scan an image at the same predefined spatial resolution. With such resolution matched reconstructions, the images should be identical except for their noise. Therefore, the PET system that produces the image with the lowest variance has the best performance. An analytical model is described to compute this variance, assuming that the PET system is (approximately) cylindrical, the imaged object is a uniform cylinder centered in the field of view, and the variance is only computed at the center of the reconstructed image. The model takes into account the solid angle covered by the detectors, the detector stopping power, the time-of-flight (TOF) resolution, the scatter fraction and the spatial resolution of the system, the attenuation and diameter of the cylinder and the desired spatial resolution of the reconstructed image. The inverse of this variance can be considered as the effective sensitivity of the system. This effective sensitivity can be calibrated based on the NEMA line source sensitivity. As a performance metric for scanning long objects, the minimum sensitivity achieved over the object is computed, with an optimal number of bed positions and optimal overlap between them. The influence of the spatial and TOF resolution on the effective sensitivity is verified with simulations.

Keywords: PET, TOF, image reconstruction, instrument optimisation

[1]Corresponding author.

Contents

1 Introduction

Current commercial PET systems include TOF systems with time resolutions between 600 and 170 ps, non-TOF systems, systems based on LYSO or BGO crystals and using different crystal sizes and thicknesses. The systems have different diameters and their axial extent ranges from 20 to 200 cm. The ongoing detector research pushing for still better timing resolution is expected to further increase this diversity. We propose an analytical model to estimate and compare the performance of different PET systems for imaging a uniform cylinder. For comparing systems, one has to specify the diameter and attenuation of the cylinder, the axial length of the region to be imaged, and the required spatial resolution of the reconstructed image, because the relative system performance depends on these parameters. This work has recently also been presented at the IEEE MIC 2023 conference [1].

2 Theory

2.1 Effective sensitivity along the scanner axis

The proposed method assumes that the PET system can be well modeled as a cylinder, possibly with gaps, and estimates the effective sensitivity (to coincident photon pairs) along the axis of the system, for imaging at a given spatial resolution. The effective sensitivity is defined here as the inverse of the variance in the center of the reconstructed image, where this reconstructed image has a predefined point spread function (spatial resolution). This definition agrees with the conventional sensitivity, because if systems A and B are identical, except that system A detects twice as many counts for the same activity in the field of view, then the effective sensitivity of A will indeed equal

twice that of B. However, effective sensitivity also incorporates other parameters that affect the variance in the reconstructed images, such a spatial resolution and time-of-flight accuracy.

By imposing a predefined reconstruction point spread function, all PET systems are forced to produce the same signal in the final image, but they may do so with a different amount of noise. Consequently, their signal to noise ratios (SNR) will be different: they have the same signal, but a different noise variance. It follows that the square of the SNR obtained with this approach is inversely proportional to the variance in the reconstructed image:

$$\text{effective sensitivity} \sim \text{SNR}^2 \sim \frac{1}{\text{VAR}} \tag{2.1}$$

The effective sensitivity can be written as

$$S_{\text{eff}} \simeq S_{\Omega,\mu}\ S_{\text{det}}\ S_{\text{TOF}}\ S_{\text{scat}}\ S_{\sigma_{\text{sysax}},\,\sigma_{\text{systrans}},\,\sigma_{\text{recon}}}, \tag{2.2}$$

where $S_{\Omega,\mu}$ combines the effects of the solid angle and the attenuation, S_{det} is the detector efficiency, S_{TOF} is the variance reduction (or effective sensitivity gain) achieved by TOF, S_{scat} is the effect of the scatter and $S_{\sigma_{\text{sysax}},\,\sigma_{\text{systrans}},\,\sigma_{\text{recon}}}$ denotes the effects of the detector resolution (axially and transaxially) and the resolution of the final reconstructed image.

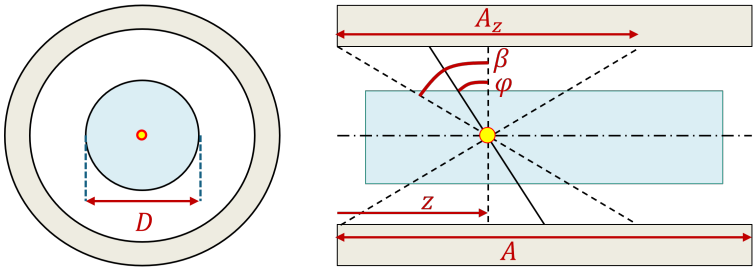

Figure 1. *Illustration of the PET parameters defined in the text and used in equation (2.3).*

The geometrical sensitivity at point z on the axis is computed as the solid angle of the cylindrical PET system, accounting for the sensitivity loss due to the gaps between the detectors:

$$S_{\Omega,\mu}(z) = S_{\text{gaps}} \int_0^{\beta} \cos(\varphi) e^{-\frac{\mu D}{\cos(\varphi)}} d\varphi \tag{2.3}$$

$$\beta = \sin^{-1}\left(\frac{A_z}{\sqrt{A_z^2 + \phi^2}}\right) \quad \text{and} \quad A_z = \min(2z, 2(A - z))$$

$$S_{\text{gaps}} = \left(\frac{\text{DetectorArea}}{\pi \phi A}\right)^2$$

where ϕ is the diameter of the PET system, μ is the linear attenuation coefficient of the cylinder, D is its diameter, A is the axial extent of the scanner and $z \in [0, A]$ is the position on the axis. A_z is the extent of the scanner that contributes to detection. These variables are illustrated in figure 1. S_{gaps} corrects for the presence of gaps between the detectors. $S_{\Omega,\mu}(z)$ is zero at $z = 0$ and $z = A$, and reaches its maximum at $z = A/2$. For TOF-PET, (2.3) must be updated by inserting (2.7) in the integrand.

The detector efficiency is computed as

$$S_{\text{det}} = \epsilon_{\text{cal}}(1 - e^{-\mu_{cp}T}) \tag{2.4}$$

where μ_{cp} is the attenuation from Compton and photoelectric interactions in the crystal and T is the crystal thickness. Because the factor between brackets assumes that any Compton interaction in the crystal results in a successful photon detection, and therefore overestimates the stopping power, the calibration factor ϵ_{cal} is introduced. This factor must be determined with a measurement; e.g. by requiring agreement between the predicted and reported NEMA line source sensitivity for each PET system.

The sensitivity gain contributed by TOF was computed for Gaussian and arbitrary TOF-kernels in [2] and [3]:

$$S_{\text{TOF},k} = c_T \int_{-\infty}^{\infty} \frac{k^2(x)}{\int_{-\infty}^{\infty} B(\xi)k(x-\xi)d\xi} dx \tag{2.5}$$

where c_T is a constant, $k(x)$ is the TOF-kernel and $B(x) = 1$ for x inside the cylinder and $B(x) = 0$ for x outside. For a system with Gaussian TOF-kernel with standard deviation σ_T and for a non-TOF system this equation reduces to [3]:

$$S_{\text{gaussTOF}} = \frac{c_T}{2\sqrt{\pi}\sigma_T} \quad \text{and} \quad S_{\text{nonTOF}} = \frac{c_T \cos(\varphi)}{D} \tag{2.6}$$

where φ is the angle between the line of response and the transaxial plane. Factor $\cos(\varphi)$ accounts for the fact that more oblique lines have a longer intersection with the cylinder. Consequently, the TOF-induced sensitivity gain equals

$$S_{\text{TOF}} = \frac{S_{\text{gaussTOF}}}{S_{\text{nonTOF}}} = \frac{D}{2\sqrt{\pi}\sigma_T \cos(\varphi)} \simeq \frac{0.664\ D}{\text{FWHM}_T \cos(\varphi)} \tag{2.7}$$

where FWHM_T is the full width at half maximum of the Gaussian TOF kernel in units of length. Equation (2.7) is inserted into (2.3) for the integration over φ (which means that the sensitivity components $S_{\Omega,\mu}$ and S_{TOF} cannot really be separated as suggested in (2.2)).

The scatter can roughly be accounted for by using

$$S_{\text{scat}} = \frac{N_{\text{true}}}{N_{\text{true}} + N_{\text{scatter}}} = 1 - \text{SF}. \tag{2.8}$$

where N_{true} and N_{scatter} are the number of trues and scatters. It is assumed that the scatter fraction SF is known. Ideally, the scatter fraction should be determined for each LOR obliqueness φ and for the chosen uniform cylinder, taking into account its attenuating material and its diameter. If that is not possible, one could use the NEMA scatter fraction as a (crude) surrogate, assuming that it is proportional to the true scatter fraction with approximately the same coefficient of proportionality for all PET systems.

The final factor quantifies the effects of the spatial resolution of the PET detectors in axial (σ_{sysax}) and transaxial (σ_{systrans}) direction, in combination with the desired spatial resolution of the reconstructed images (σ_{recon}). We assume that all corresponding point spread functions are Gaussians. It is known that in 2D PET, the variance in the reconstructed image is proportional to

$1/\sigma_p^3$, where σ_p is the standard deviation of a 2D Gaussian postsmoothing mask (see e.g. [2, 3]). Smoothing a set of parallel slices in the plane direction further reduces the variance with factor $1/\sigma_p$, producing a factor of $1/\sigma_p^4$ for 3D imaging with a 2D PET system (with septa). Extending the work of [2] to fully 3D PET with complete 4π angular coverage, one also finds this dependence on $1/\sigma_p^4$, but in this case the variance reduction is a factor $\pi^2/8 \simeq 1.23$ higher. This same factor was found for non-TOF PET in [4]. Since real PET systems do not have full 4π angular coverage, using the 2D PET + axial smoothing expression should produce an error smaller than 23%. Consequently, if the system has a transaxial resolution of σ_{systrans} and an axial resolution of σ_{sysax}, we have to apply 2D smoothing with $\sqrt{\sigma_{\text{recon}}^2 - \sigma_{\text{systrans}}^2}$ in the transaxial plane and with $\sqrt{\sigma_{\text{recon}}^2 - \sigma_{\text{sysax}}^2}$ in the axial direction to obtain a 3D Gaussian point spread function with standard deviation σ_{recon} in the final image. Consequently

$$S_{\sigma_{\text{sysax}}, \sigma_{\text{systrans}}, \sigma_{\text{recon}}} = (\sigma_{\text{recon}}^2 - \sigma_{\text{systrans}}^2)^{1.5} (\sigma_{\text{recon}}^2 - \sigma_{\text{sysax}}^2)^{0.5} \tag{2.9}$$

which confirms that PET systems with higher resolution have a higher effective sensitivity, in particular when aiming for image reconstruction with high spatial resolution. Equation (2.9) is only valid if $\sigma_{\text{TOF}} \gg \sigma_{\text{sys}}$, which is the case for current PET systems. The system resolution can be derived from point source sinograms or listmode data, or estimated from the corresponding FBP reconstructions.

2.2 Minimum sensitivity over a (long) object

For scanning a long object, we consider scanning the object in N bed positions with an overlap V between consecutive bed positions. The scan time per bed position equals T/N, where T is the total acquisition time. This implies that the time for moving the bed is negligible, but if that time is known it can easily be accounted for. For scanning an object with a particular PET system, N and V are optimized by maximizing the minimum sensitivity achieved over the object, as illustrated with the blue line in figure 2. The sensitivity for a single bed position is computed as outlined in the previous section, and the optimization was done by incrementing N, numerically optimizing V, and selecting the combination (N, V) that achieved the highest minimum sensitivity. We use this highest possible minimum sensitivity as the performance metric for imaging an object of a particular length.

3 Numerical verification

A systematic evaluation with 3D simulations is still to be done. Equation (2.5) has been verified in [3]. Here we compare the analytical prediction for three 2D PET systems with different TOF-resolutions (15 and 30 mm, or 100 and 200 ps) and different transaxial detector resolutions (2, 3 and 6 mm), for imaging a uniform disk (20 cm diameter) at different spatial resolutions. For the simulations and reconstructions, we used an image of 200 × 200 pixels and a pixel size of 1.33 mm × 1.33 mm. All image reconstructions were done with 40 MLEM iterations (which results in good convergence for these excellent TOF-resolutions), without detector resolution compensation. The image resolution was varied with Gaussian postsmoothing. From noise-free simulations of the disk with and without the addition of a local impulse (10% activity increase in a central pixel), the

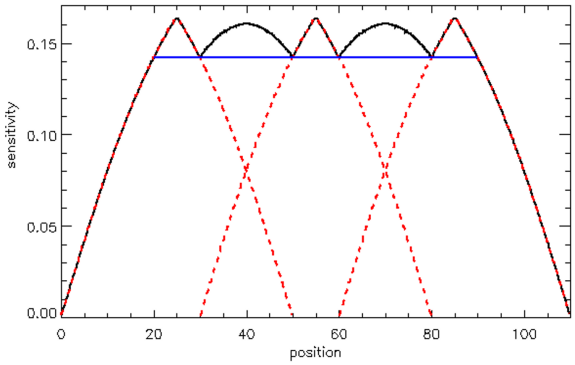

Figure 2. *Acquisition with 3 bed positions. Red dashed lines show the sensitivity from each bed position, the solid black line shows the overall sensitivity and the blue line indicates the minimum sensitivity obtained along the scanned object.*

image resolution was determined. From 40 noisy sinograms for each system, the variance in the reconstructed image was determined, by computing the mean pixel variance in a central region with 6 cm diameter.

4 Results

Fig. 3 compares the effective sensitivities observed in the simulations to those predicted by the proposed model, as a function of the spatial resolution in the reconstructed image. The system with the best detector resolution (2 mm) and the best TOF resolution (30 mm) outperforms the other two systems as expected (pink curves in fig. 3). For high resolution imaging, the system with 3 mm detector resolution (red curves) has a higher effective sensitivity than the system with 6 mm resolution (black curves). However, for imaging at lower resolution, the system with 6 mm detector resolution performs better, because of its superior TOF resolution. These two systems have equal sensitivity for imaging at a resolution of 9 mm FWHM. A single scale factor was fitted to scale the three predictions to the three observed SNR^2 curves. For all systems, an excellent agreement between the predictions and simulations is obtained.

5 Discussion

The proposed analytical model estimates the effective sensitivity of a particular PET system. The model has obviously several limitations. The most important limitation is that it only holds for the center of a uniform cylinder. The diameter and the attenuation of the cylinder can be chosen, but it is assumed that the activity is uniform. The model is useful under the assumption that, if a PET system is superior for imaging uniform cylinders of various diameters, it is very likely to be also superior for imaging non-uniform attenuating objects, including tracer distributions in patients.

The model relies on cylindrical symmetry of the PET system, which is reasonable for most current clinical PET systems. However, there is an increasing interest in organ-dedicated PET systems, which are often not cylindrical. Moreover, the continuously improving time-of-flight resolution reduces the need for complete angular sampling, which makes various non-conventional PET geometries increasingly attractive. Extending the model for non-cylindrical systems will make the mathematics more complicated, and possibly intractable for some geometries of interest.

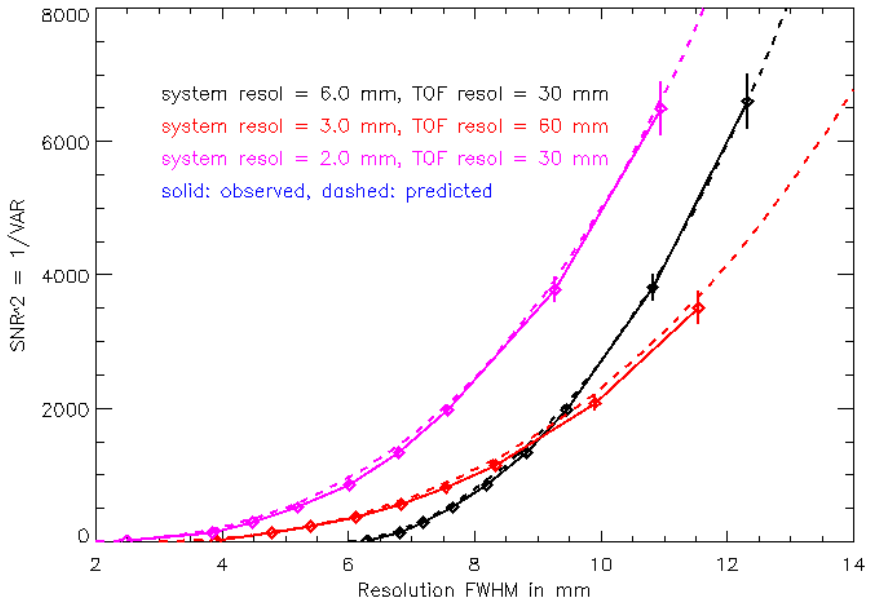

Figure 3. *Plot of 1/variance (= SNR^2) as a function of the resolution of the reconstructed image, as obtained from the simulation study (solid lines). The dashed lines show the corresponding analytical predictions. The error bars correspond to* ±2 *standard deviations.*

On the other hand, thanks to these simplifications, an analytical model can be derived, which provides insight and requires a negligible computation time. We believe it is a useful complement to Monte Carlo simulation, which requires more computation time and produces more accurate results but less insight.

A systematic validation for 3D PET with septa and fully 3D PET is still to be done. As mentioned above, an approximation was introduced which makes the current model less accurate for PET systems with higher angular coverage. However, this and some other approximations can be avoided if one is willing to accept the increased complexity. The development and validation of more accurate analytical models for the effective sensitivity is ongoing.

Using the results of [2, 3], the effect of TOF on the effective sensitivity could be included. Interestingly, these same equations also include the effect of the reconstruction point spread function, which produced, after introducing some approximations, equation (2.9). This shows that improving the detector resolution increases the effective sensitivity, even when a less good resolution is required in the final images (figure 3). This relation between detector resolution and effective sensitivity agrees with results in [5, 6], where it was found that if the system resolution increases, the same final image quality can be obtained with fewer counts (shorter scan time or reduced dose).

6 Conclusion

An analytical model for the effective sensitivity of PET-systems is proposed, which is based on the imaging performance for a uniform (radioactive) cylinder. The model takes into account the contributions of the solid angle covered by the detectors, the detector stopping power, the time-of-flight resolution, the scatter fraction, the spatial resolution of the system, the attenuation and diameter of the uniform cylinder, and the axial extent and the spatial resolution of the reconstructed

image. With this model, the performance of very different PET systems can be compared for a particular imaging task.

Acknowledgments

This work was supported in part by the Research Foundation - Flanders (FWO) under grant G062220N. The authors thank Floris Jansen, Tim Deller and Matthew Spangler-Bickell (GE), and Michel Defrise (VUB), for many discussions on this topic.

References

[1] J Nuyts, SA Zaman Pour, S Noë, G Schramm, A Rezaei, "An analytical model for comparing the effective sensitivity of different PET systems", *IEEE NSS MIC*, 2023; M10-092.

[2] T Tomitani. "Image reconstruction and noise evaluation in photon time-of-flight assisted positron emission tomography". *IEEE Trans Nucl Science*, 1981; NS-28: 4582-4589.

[3] J Nuyts, M Defrise, S Gundacker, E Roncali, P Lecoq. "The SNR of positron emission data with Gaussian and non-Gaussian time-of-flight kernels, with application to prompt photon coincidence". *IEEE Transactions on Medical Imaging.*, 2022.

[4] M Defrise, DW Townsend, F Deconinck. "Statistical noise in three-dimensional positron tomography", *Phys Med Biol* 1990, 35: 131-138.

[5] G Muehllehner, "Effect of resolution improvement on required count density in ECT imaging: a computer simulation", *Phys Med Biol* 1985, 30 (2): 163-173.

[6] S Surti, AR Shore, JS Karp, "Design study of a whole-body PET scanner with improved spatial and timing resolution", *IEEE Trans Nucl Sci* 60 (5): 3220-3226.